Mitigation of Flow-Induced Cylinder Noise Through the Control of Sound Diffraction

(Article begins on next page)

Mitigation of Flow-Induced Cylinder Noise Through the Control of Sound Diffraction

Riccardo Zamponi*
Delft University of Technology, 2629HS Delft, The Netherlands
von Karman Institute for Fluid Dynamics, Waterloosesteenweg 72, B-1640 Sint-Genesius-Rode, Belgium

Francesco Avallone†
Politecnico di Torino, Corso Duca degli Abruzzi 24, 10129 Torino, Italy

Daniele Ragni‡ and Sybrand van der Zwaag§
Delft University of Technology, 2629HS Delft, The Netherlands

The sound emitted by the flow past a circular cylinder can be described by a quadrupole placed at the outbreak location of the shedding instability and diffracted surface into the far field by the body with a dipolar directivity. This mechanism is greatly stabilized for a cylinder coated with a porous material, which features a substantial downstream shift of the onset location of the shed vortices that leads, in turn, to a reduction in the efficiency of the sound scattering and consequent noise mitigation. In this research, a novel design for a porous treatment of the cylinder based on the enhancement of this effect is proposed. Far-field acoustics tests were performed at the Delft University of Technology for Reynolds numbers based on the cylinder diameter ranging in the subcritical regime. The outcomes of the analysis demonstrate that, when the aft part of the flow-permeable coating is modified to make the internal flow more streamlined, an additional sound attenuation of up to $10\,\mathrm{dB}$ is achieved in comparison with a uniform porous cover. Moreover, a significant noise decrease of up to $10\,\mathrm{dB}$ and potential drag reduction are obtained if these components are connected to the bare cylinder without the use of a porous coating. This result can open up interesting opportunities to design disruptive and more optimized sound-mitigation solutions.

I. Introduction

Tʜᴇ aerodynamic noise produced by a circular cylinder immersed in a transverse flow, referred to as Aeolian tone, affects a large number of engineering applications, including landing-gear systems and high-speed trains. This noise source is associated with the shedding of vortical structures that periodically detach from opposite sides of the cylinder surface [1]. Decreasing the unsteadiness of this so-called von Kármán street has a beneficial effect on the emitted sound [2].

One of the most promising passive flow-control strategies to reduce the Aeolian tone by controlling the vortex shedding is to coat the surface of the cylinder with a porous material. Several experimental and numerical investigations have been carried out in the last decade to analyze the noise-mitigation performance achievable with a flow-permeable coating. The first study on the topic was performed by Sueki *et al.* [3], who demonstrated the effectiveness of this technological solution in reducing aerodynamic sound by suppressing the unsteady motion of the shed vortices that, in turn, decreases the aerodynamic force fluctuations on the surface. This stabilization effect of the oscillating wake was explained by Naito and Fukagata [4] in terms of slip velocity and fluid energy. Liu *et al.* [5] showed that, besides the noise attenuation, the integration of a metal-foam cover decreases the vortex-shedding peak towards lower frequencies and narrows its bandwidth, with an effect that increases along with the thickness, porosity, and average pore dimension of the permeable layer. Similar results were obtained for cylinders coated with metal foam by Aguiar *et al.* [6]. Showkat Ali *et al.* [7] observed that the most significant effect of the porous coating of the cylinder on the flow field is to shift the vortex-formation region downstream and decrease the turbulence kinetic energy. Moreover, Geyer *et al.* [8] tested several

---

*Assistant Professor, Department of Flow Physics and Technology, r.zamponi@tudelft.nl, AIAA Member

†Assistant Professor, Department of Mechanical and Aerospace Engineering, francesco.avallone@polito.it, AIAA Member

‡Associate Professor, Department of Flow Physics and Technology, d.ragni@tudelft.nl, AIAA Member

§Professor Emeritus, Department of Novel Aerospace Materials, S.vanderZwaag@tudelft.nl, AIAA Member

porous media and showed that materials that are highly permeable to air yield the best noise mitigation. Comparable findings were obtained by Geyer [9], who estimated the key parameters acting on the vortex-shedding tonal noise using the method of linear regression.

In addition, novel solutions for integrating porosity based on structured 3D-printed covers were recently proposed. Arcondoulis *et al.* [10] designed a structured porous coating whose porosity and permeability can be modified independently. They demonstrated that such a design could yield comparable vortex-shedding-tone suppression and frequency shift in the acoustic power spectral density to that obtained with randomized permeable foams characterized by the same parameters. Besides the possibility of investigating the flow field within the porous medium, thanks to the optical access [11], this structured coating offers the advantage of integrating non-uniform innovative solutions where the porosity varies along the span or circumference of the porous cover [12, 13]. A similar design was also suggested by Bathla and Kennedy [14], who evaluated the suitability of masked stereolithography (MSLA) 3D printers for manufacturing coatings based on repeated unit cells made of self-supporting lattices. Notably, they showed that employing partial covers with a helicoidal or spaced shape results in comparable flow-stabilization performance to that of a full coating while considerably reducing the material utilization.

This study proposed a novel and more effective design for a nonuniform coating of a cylinder based on the alteration of sound scattering. This solution has been inspired by recent findings from the authors [15], who demonstrated that, for the whole frequency spectrum for which the noise related to the flow recirculation within the pores of the material does not prevail, the dominant sound sources produced by the flow past a circular cylinder are located in the wake of the body, at the onset of the vortex-shedding instability. This region is associated with the origin of a quadrupolar source that radiates into the far field and is scattered by the body surface. The efficiency of such a diffraction mechanism is expected to decrease exponentially with the increasing distance from the body, as typically occurs for acoustically compact cases [16]. Therefore, maximizing the downstream shift of the vortex-shedding onset position represents a valid design criterion for the aeroacoustic treatment of the cylinder. To verify the effectiveness of this technological solution, several coating prototypes based on the modification of existing metal-foam covers have been manufactured and tested at the A-Tunnel facility of the Delft University of Technology (TU Delft) by means of far-field acoustic measurements.

The manuscript is structured as follows. The measurement setup arranged for the experimental campaign is described in Section II. In Section III, the main aeroacoustic results are outlined and discussed, highlighting the connection between the alteration and the sound scattered by the body and the noise mitigation provided by the proposed innovative coatings. Finally, the conclusions are drawn in Section IV.

II. Methodology

A. Wind-tunnel facility and cylinder specimen

The A-tunnel facility of the TU Delft, where the measurement campaign described in this paper has taken place, is a vertical open–jet wind tunnel placed in an anechoic chamber equipped with Flamex Basic acoustic absorbing foam that results in a cutoff frequency of 250 Hz [17]. The outlet nozzle of the vertical tunnel is installed at the exit of the contraction, has a height of 1 m, and features a rectangular exit plane having a contraction ratio of 42 to 1, a span of $s = 0.250$ m, and a width of $w = 0.400$ m. The circular cylinder specimens are supported by two side plates, which guide the flow from the outlet nozzle and have a length equal to s. A schematic of the experimental arrangement is illustrated in Section II.A, where the reference system used for the presentation of the results is reported. Specifically, the x-axis is aligned with the streamwise direction, the z-axis is aligned with the span of the specimen, and the y-axis is oriented in order to form a right-handed coordinate system. The origin is placed at the midspan of the trailing edge of the cylinder.

Several configurations have been tested in this analysis: a bare cylinder, or baseline, a cylinder coated with a porous material, and different non-uniform covers designed as modifications of the first two. As indicated in Zamponi *et al.* [15], the diameter d of the inner specimen has been maintained constant to model the integration of external material into an existing device. The outer diameter D of the covered specimen is hence given by the coating thickness t, according to $D = d + 2t$. The geometry of the tested configurations has been then designed to allow the vortex shedding to occur [18], minimize the blockage exerted by the body, and produce a vortex shedding above the cutoff frequency of the anechoic facility. Moreover, the thickness of the cover should be large enough for the flow to penetrate the porous medium. The resulting dimensions have been $d = 20$ mm, $D = 30$ mm, and $t = 5$ mm, leading to aspect ratios of $L/d = 12.5$ and $L/D = 8.33$.

The measurements have been carried out at free-stream flow velocities in the subcritical regime ranging from
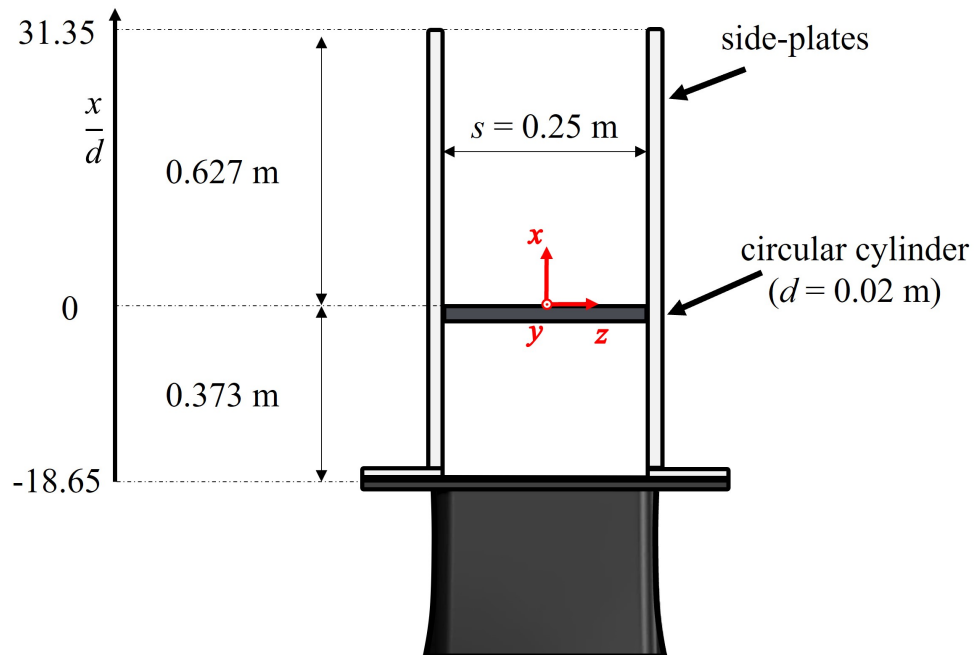
Fig. 1 Test section showing the outlet nozzle, side plates, and cylinder specimen, including the reference system considered for the presentation of the results.

$U_\infty = 25 \, \text{m s}^{-1}$ to $U_\infty = 50 \, \text{m s}^{-1}$ that provide Reynolds numbers based on the inner cylinder diameter of $Re_d = 3.4 \times 10^4$ and $Re_d = 6.8 \times 10^4$, respectively. The flow speed is measured through a Pitot static tube plugged into a Mensor DPG 2400 pressure gauge and having an accuracy of 0.03 % of the read value. From previous qualification analyses, the mean velocity in the streamwise direction was found to be uniform within 0.6 % independently of the free-stream velocity, whereas the turbulence intensity of the clean flow was below 0.1 % for the entire range of operative velocities [17].

B. Porous coating

The porous coating is made of a Nickel Ni open-cell metal foam manufactured through the electrodeposition of pure Nickel on a polyurethane foam, which results in a homogeneous microstructure based on a dodecahedron-shaped cell. This material has already been used for analogous measurement campaigns in the literature [3, 6, 10]. The metal foam possesses a nominal cell diameter of 10 PPI, the PPI being a non-SI unit usually employed as an indication of the number of pores per inch, and a porosity φ, which is defined as the ratio of the void volume to the total volume, of 95 %. These values agree well with those considered in the literature results mentioned in Section I.

The characterization of the porous media has been performed using the experimental rig described in [19]. This technique consists of least-squares fitting the Hazen-Dupuit-Darcy quadratic equation [20]

$$\frac{\Delta p}{t_s} = \frac{\mu}{K} v_d + \rho C v_d^2, \tag{1}$$

Δp being the pressure drop across a homogeneous porous material sample with thickness t_s, μ the fluid dynamic viscosity, v_d the Darcian velocity, which is determined as the ratio of the volumetric flow rate to the cross-section area of the material sample, and K and C the static permeability and form coefficient of the porous medium, which account for pressure losses due to viscous and inertial effects, respectively. In addition, the term $R = \Delta p/(t_s v_d)$ denotes the static air-flow resistivity of the material. An ensemble of 20 values of pressure drop, corresponding to Darcian velocities ranging between $0 \, \text{m s}^{-1}$ and $2.5 \, \text{m s}^{-1}$, are considered for fitting Eq. (1).

Two pressure ports are placed 50 mm upstream and downstream of the test section and are connected to a Mensor DPG 2101 pressure gauge featuring an accuracy of 2 Pa. The volumetric flow rate is controlled through an Aventics pressure regulator and evaluated by a TSI 4040 volumetric flow meter that is located upstream of the pipe and has an accuracy of 2 % of the read value.

3

Table 1   Measured properties for the metal-foam samples. Quantities in parentheses refer to the nominal values provided by the manufacturer.

PPI [-]	φ [%]	R [N s m^{-4}]	K [m^2]	C [m^{-1}]
(10)	(95)	4.148×10^1	4.371×10^{-7}	1.103×10^2

The porous-material samples are 55 mm metal-foam disks inserted in a hollow aluminum cylinder, which is placed in the test section. A parametric study on t_s has been carried out to prevent the occurrence of entrance or exit effects on the measured pressure drop, which may prevail if the thickness of the sample is too small [21, 22]. Hence, t_s has been varied between 40 mm and 120 mm. The convergence in the values of K and C has been found for the thickest samples, hinting that spurious effects can be assumed negligible. The outcome of the characterization is listed in Table 1.

C. Modifications of the porous coating

As mentioned in Section I, the noise-reduction mechanism of the porous treatment of a bluff body is associated with the downstream shift of the onset location of the vortex shedding and the consequent alteration in sound diffraction [15]. In the present section, several modifications of the bare and coated cylinders that emphasize this effect are proposed. A graphical overview of all tested covers and the related nomenclature is given in Fig. 2a.

Two different sleeves, denoted as *insert* and *tail*, have been designed to be rigidly connected to the leeward part of the bare cylinder specimen. The former is shaped as an annulus sector beveled in correspondence with the outer edges and projected onto the spanwise direction, the annulus being characterized by the same geometry as the porous coating. The latter shares the basis of the insert but, in this case, the sides of its section extend beyond the outer circumference arc until they intersect (see Fig. 2a).

Furthermore, two configurations have been 3D printed using Polyamide 12 for each sleeve, namely a solid, which is impermeable to flow, and a porous one, which features perforations oriented along the azimuthal direction with respect to the cylinder center. The diameters of the perforations are 1.8 mm and 3 mm for the insert and tail, respectively. No communication in the radial direction is allowed here. The geometrical characteristics of the manufactured pieces are illustrated in Fig. 2b.

A sector shaped as the negative of the insert has been cut from the metal-foam cover with the purpose of accommodating the components into the coated cylinder. The resulting sleeve can then be slid along the surface to form a sort of nonuniform porous coating. The idea behind this design is to provide a more streamlined shape for the internal flow within the permeable medium to follow. The ejection of less disturbed flow from the leeward part of the body can move the vortex-shedding onset location more downstream and, in turn, further decrease the efficiency of the sound diffraction by the surface, as mentioned in Section I.

D. Far-field acoustic measurements

A G.R.A.S. 40 PH analog free-field microphone with integrated constant-current power amplifiers is used for the far-field acoustic measurements. The transducer has a diameter of 0.007 mm and a length of 0.059 mm, and features a flat frequency response within ±1 dB from 50 Hz to 5 kHz and within ±2 dB from 5 kHz to 20 kHz. It is connected to a data acquisition system comprising 4 NI PXIe-4499 Sound and Vibration Modules with a 24 bits resolution and a 204.8 kHz maximum sampling rate. The boards are controlled by a NI RMC-8354 computer via a NI PXIe-8370 board. The microphone, which is located at $(x, y, z) = (5\,d, 59.25\,d, -0.25\,d)$, has been calibrated in amplitude using a G.R.A.S. 42AG pistonphone, emitting a sinusoidal wave of 94 dB at 1 kHz.

For each cylinder configuration, the data have been acquired at a sampling frequency of 102.4 kHz for 20 s. 5 free-stream Reynolds numbers have been considered, namely $Re_d = 3.4 \times 10^4$, 4.1×10^4, 4.8×10^4, 5.4×10^4 and 6.8×10^4. The power spectral densities of the acoustic signals have been calculated by means of the Welch method [23], with blocks of 2^{13} samples windowed through a Hanning weighting function that have 50 % of data overlap, hence delivering a frequency resolution of 12.5 Hz. For these parameters, the corresponding random error considering a 95 % confidence interval is estimated to be in the order of 0.8 dB [24].
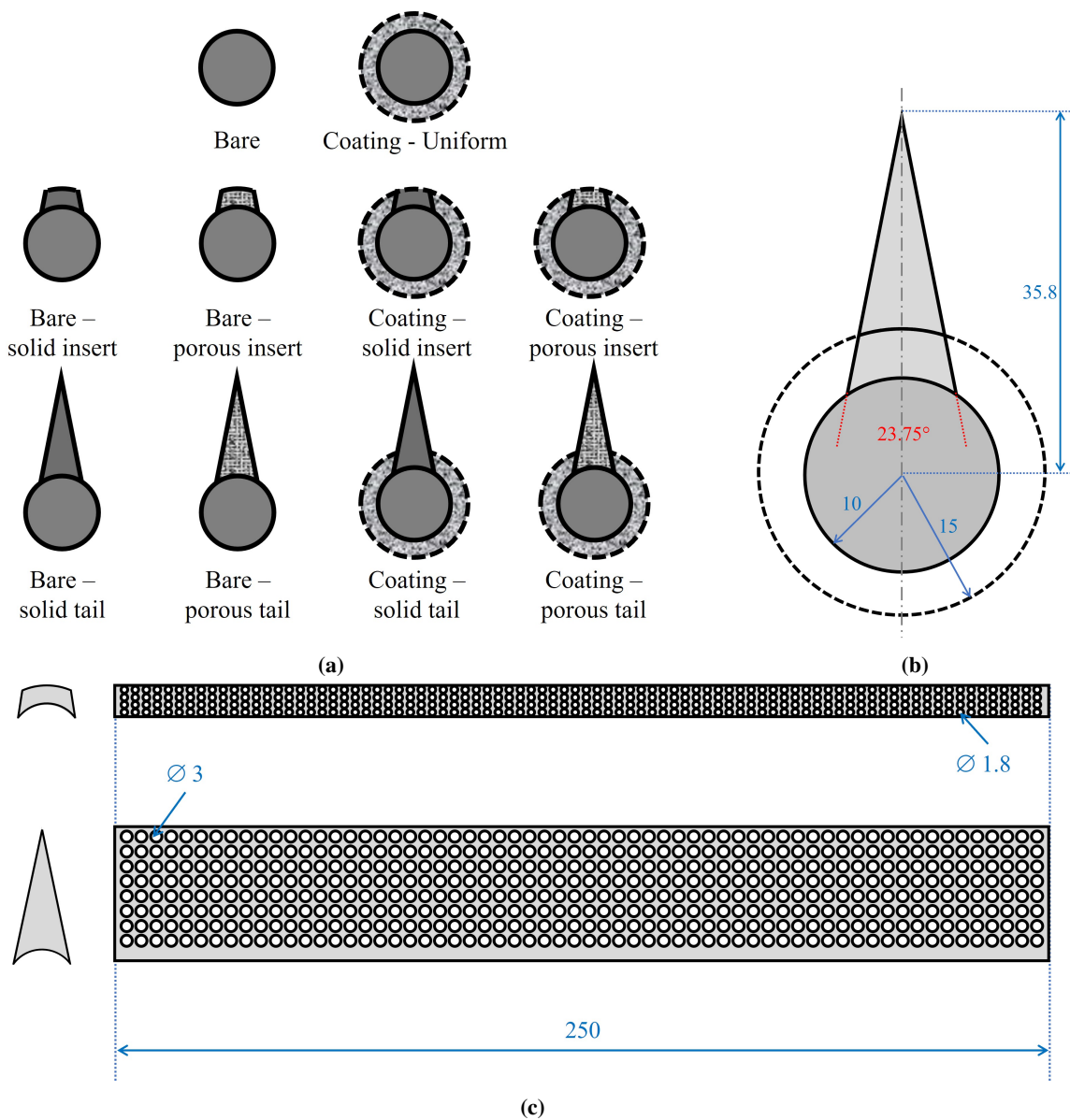
Fig. 2 **(a) Overview and nomenclature of the tested configurations based on the bare and coated cylinders. (b) Geometrical dimensions of the coating modifications. (c) Schematic of the porous insert and tail. Distances are given in** mm.

III. Results and discussion

A. Sound pressure levels

The sound-pressure levels L_p of the signal acquired by the central microphone of the array, placed at an observation angle of approximately $\pi/2$ with respect to the stagnation streamline, are plotted in Figs. 3 and 4 for the cylinder configurations depicted in Fig. 2a and evaluated at different free-stream Reynolds numbers. Each figure refers to a different modification procedure: the former includes the metal-foam coating, whereas the latter does not. The frequency spectra are presented at a reference distance of 1 m and in function of the Strouhal number based on d and U_∞. Consistent results with those of Zamponi *et al.* [15] are obtained for the baseline and the cylinder uniformly coated with the 10 PPI metal foam: the porous treatment is effective in mitigating noise, with a trend that is mostly independent of the flow velocity. The difference in the outer diameter yields a shift of the tonal peak linked to the vortex
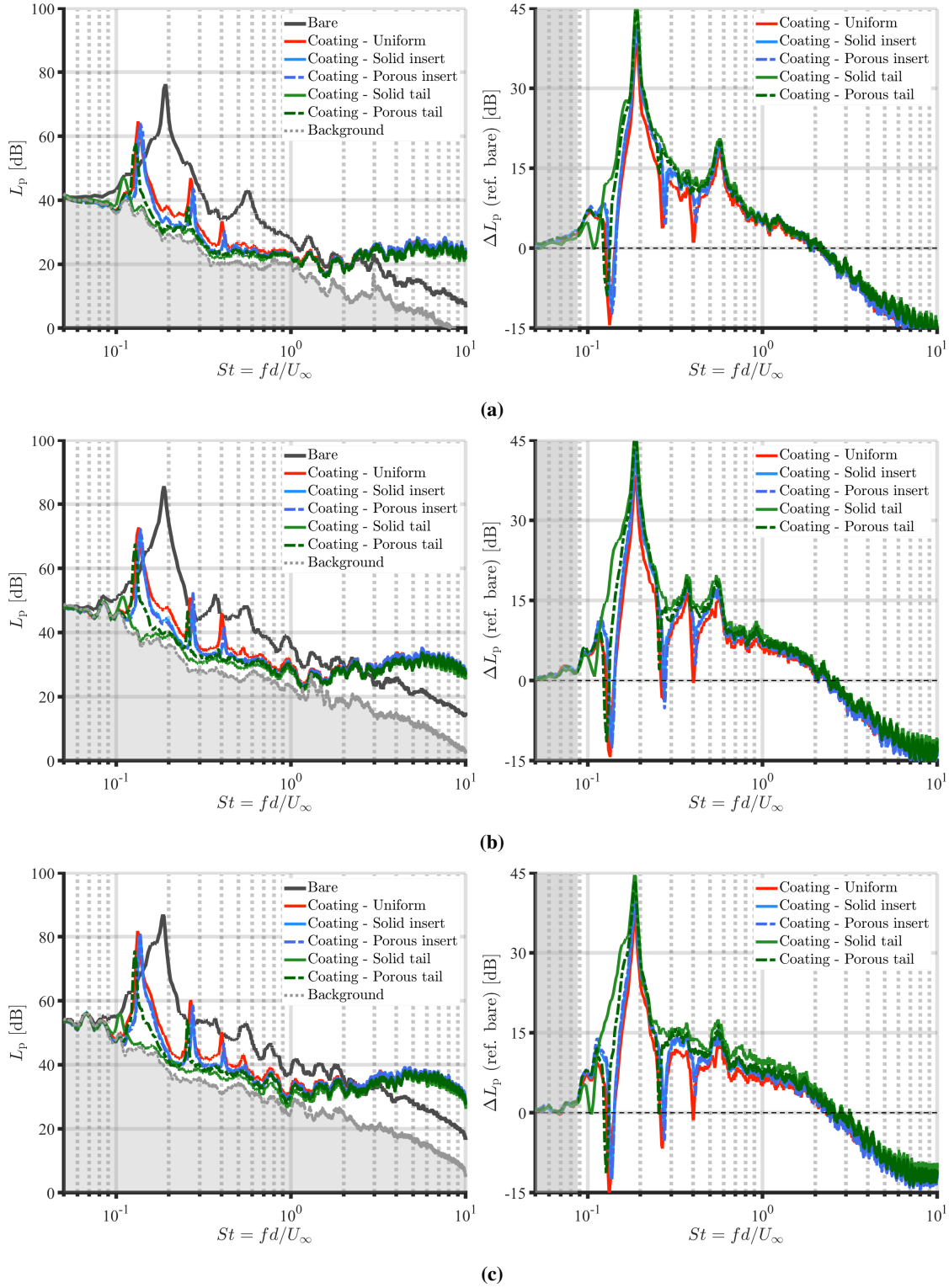
5

Fig. 3 **Relative (with respect to the uniformly coated cylinder) sound pressure levels for the cylinder configurations without the porous coating (left-hand group in Fig. 2a) at (a)** $Re_d = 4.1 \times 10^4$**, (b)** $Re_d = 5.4 \times 10^4$**, and (c)** $Re_d = 6.8 \times 10^4$ **measured by the central microphone of the array and computed with a reference pressure of** $p_{\mathbf{ref}} = 20\,\mu\mathrm{Pa}$**. The gray-tinted area on the right-hand side denotes the region in which the signal-to-noise ratio for the baseline is lower than** $3\,\mathrm{dB}$**.**
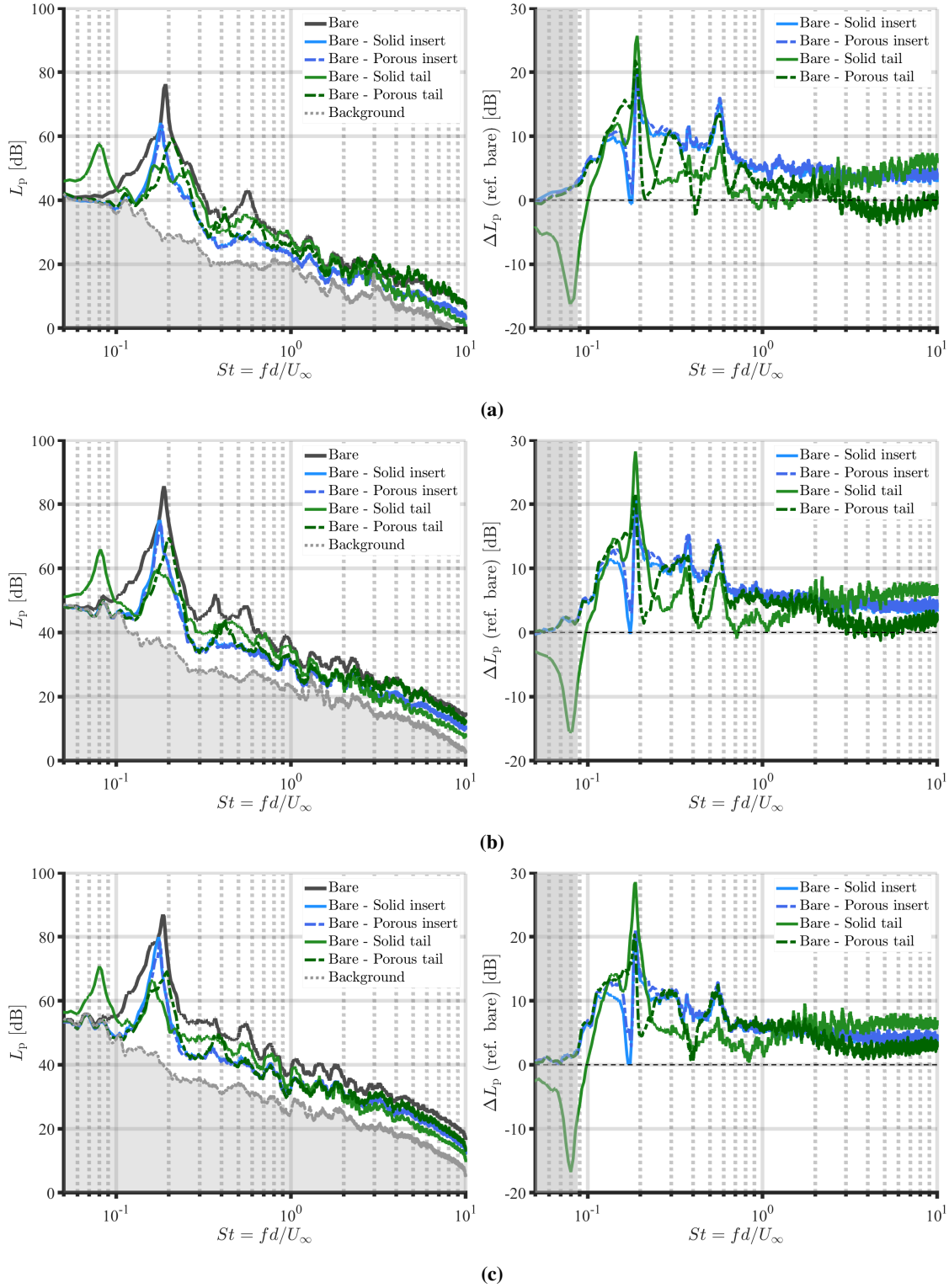
6

Fig. 4 Absolute (on the left) and relative (on the right) sound pressure levels for the bare cylinder and cylinder configurations without the porous coating (left-hand group in Fig. 2a) at (a) $Re_d = 4.1 \times 10^4$, (b) $Re_d = 5.4 \times 10^4$, and (c) $Re_d = 6.8 \times 10^4$ measured by the central microphone of the array and computed with a reference pressure of $p_{\text{ref}} = 20\,\mu\text{Pa}$. The gray-tinted area on the right-hand side denotes the region in which the signal-to-noise ratio for the baseline is lower than $3\,\text{dB}$.
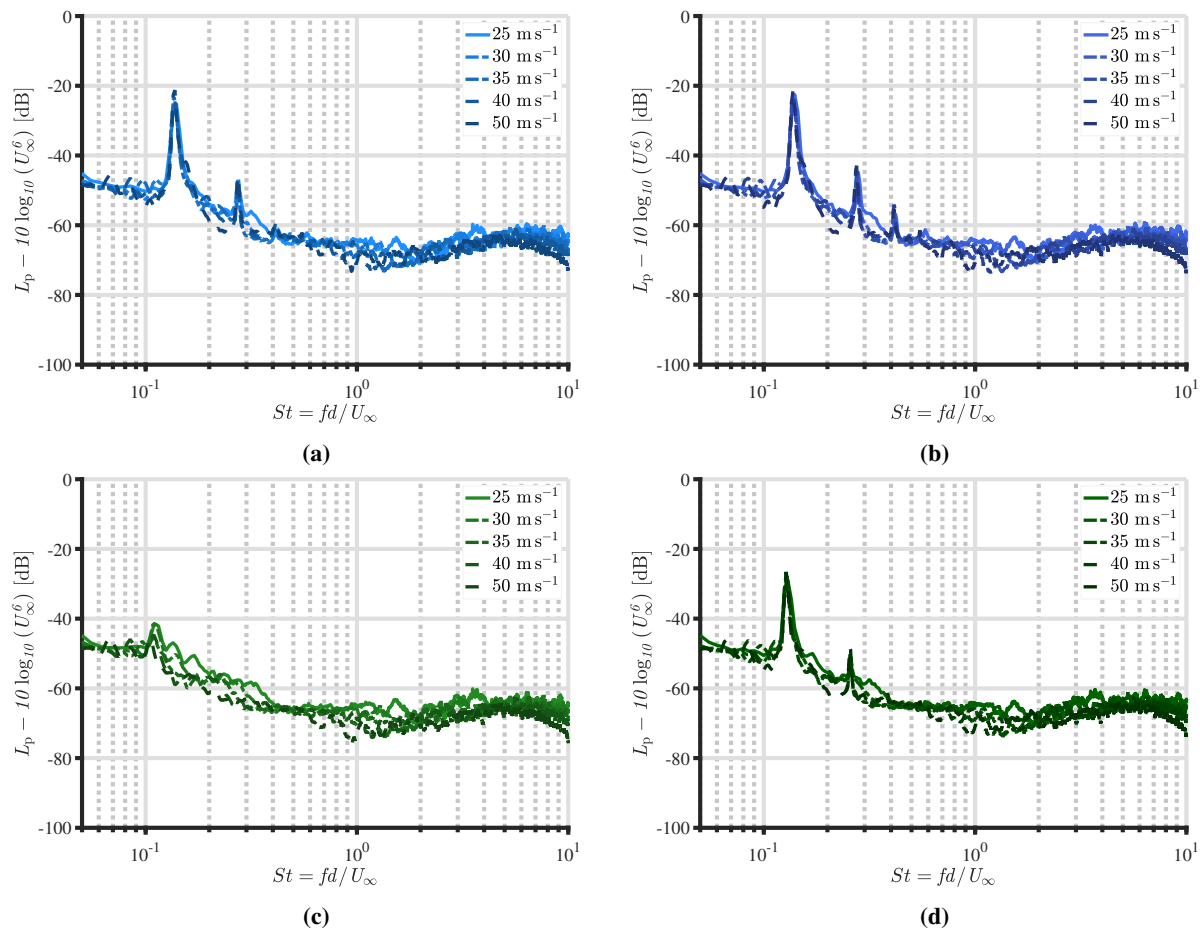
Fig. 5 Sound pressure levels at different free-stream flow velocities for the coated cylinder integrated with the (a) solid insert, (b) porous insert, (c) solid tail, and (d) porous tail measured by the central microphone of the array and computed with a reference pressure of $p_{\text{ref}} = 20\,\mu\text{Pa}$. The spectra are scaled with the sixth power of the flow velocity.

shedding at $St = 0.185$, which is in agreement with previous measurements involving circular cylinders tested in the same experimental setup [25, 26], towards lower frequencies and a substantial attenuation of its amplitude, resulting in peak-to-peak reductions of up to 11 dB. An effective diameter of $D_{\text{eff}} = 0.950\,D$ can be estimated in this case. Concerning the broadband-noise range, a significant reduction of up to approximately 10 dB is found. However, the aeroacoustic benefit of the coating reduces with increasing frequency due to the occurrence of noise induced by the recirculating flow within the metal-foam pores [15]. The tradeoff between sound decrease and increase is at $St \approx 2$, while, at $St \approx 10$, the noise increment amounts to about 15 dB.

Overall, the presence of the insert (see Fig. 2a) results in an additional noise decrease of up to 4 dB in the broadband range, especially in the region between the vortex-shedding peak and its first harmonic. No notable difference between the solid and porous inserts is found, possibly due to the fact that the perforations are oriented normally to the internal-flow direction in the leeward part of the coating and have a negligible effect on the flow ejection in the near-wake region. At high frequencies, the sound-increase trend overlaps with that of the uniform coating, hinting that noise due to the flow-recirculation within the pores is generated on the metal-foam surface in the front part of the body and is, therefore, not affected by the modifications in the back.

When the tail is integrated into the porous coating, the aeroacoustic performance of the treatment considerably improves. With the porous configuration, consistent mitigation of up to 10 dB is achieved for both tonal and broadband noise ranges. Moreover, the sound increase due to the flow recirculation is also slightly attenuated. Such trends are even more emphasized when the coated cylinder is fitted with a solid tail. In this case, the peak-to-peak reduction amounts
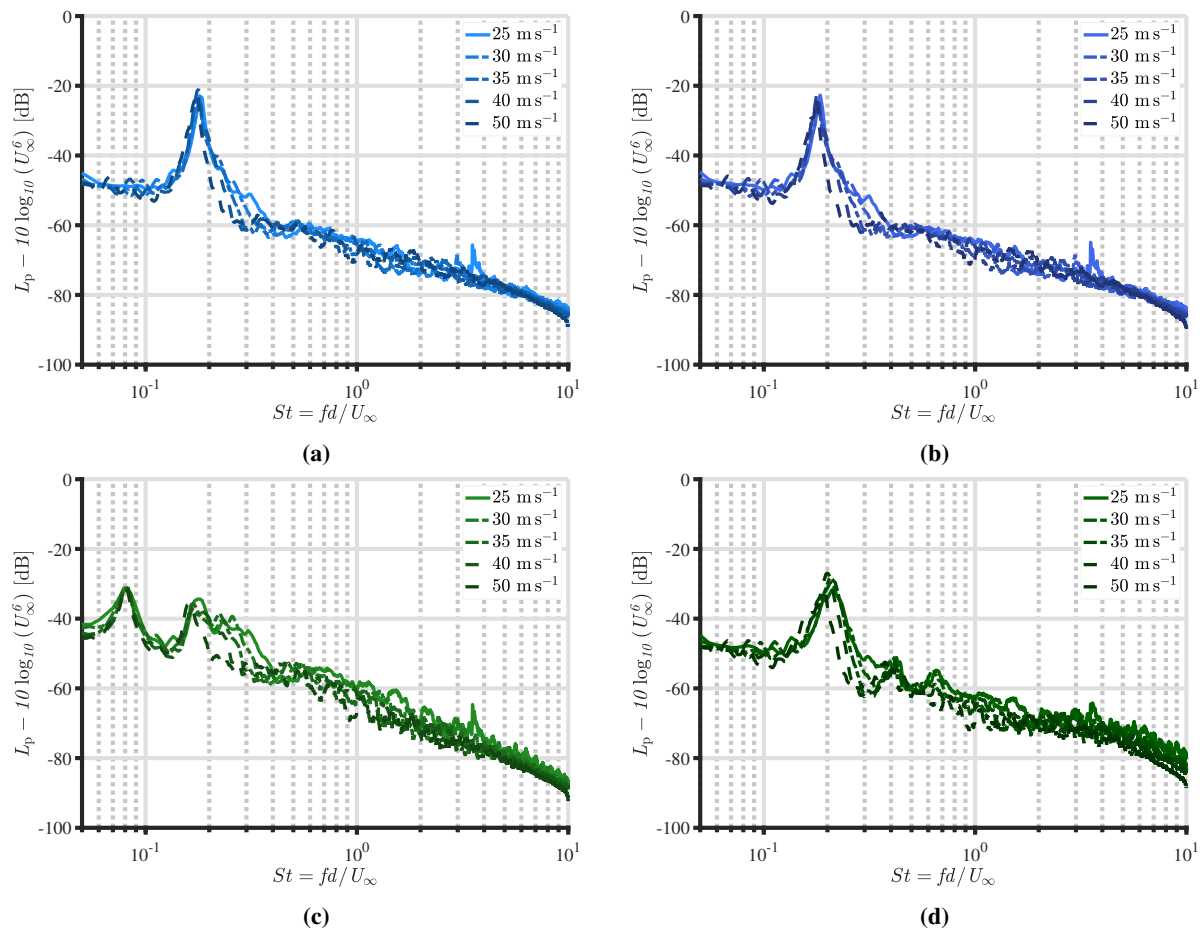
Fig. 6 Sound pressure levels at different free-stream flow velocities for the bare cylinder integrated with the (a) solid insert, (b) porous insert, (c) solid tail, and (d) porous tail measured by the central microphone of the array and computed with a reference pressure of $p_{\mathbf{ref}} = 20\,\mu$Pa. The spectra are scaled with the sixth power of the flow velocity.

to 18.5 dB with respect to the uniform coating, which, in turn, leads to a decrease of 29.2 dB if compared with the bare configuration. Interestingly, the Strouhal number at which the vortex shedding occurs is shifted towards lower frequencies, yielding $D_{\text{eff}} = 1.139\,D$. The presence of a solid plane that guides the flow ejected by the porous coating is most likely able to stabilize further the cylinder wake, with an effect similar to that produced by splitter plates [27].

The results shown above demonstrate that a nonuniform coating effectively reduces aerodynamic noise. Nevertheless, integrating a flow-permeable cover, which may also lead to generating additional sound sources associated with the presence of nonzero Reynolds stresses at the cylinder surface [28, 29], is not indispensable to achieve this effect. As illustrated in Fig. 4, consistent sound attenuation is obtained even when the inserts and tails are fitted to the cylinder in the absence of the metal-foam cover. With the former, a ΔL_p of approximately 10 dB for $0.1 < St < 0.6$ and around 5 dB for $St > 0.6$ is achieved. Similar to the previous case, no significant difference between the solid and porous insert configurations can be found. In contrast, the presence of perforations in the latter considerably affects the noise levels produced by the flow past the cylinder. On the one hand, the porous tail provides higher sound reductions in the vicinity of the Aeolian tone than the inserts but worse performance in the high-frequency range, especially for $St > 1$, probably due to surface-roughness noise [30]. This effect is more prominent for lower velocities. On the other hand, the solid tail substantially shifts the vortex-shedding peak towards lower frequencies, hinting at an alteration in the flow physics associated with this configuration.

B. Noise-spectra scaling

The L_p trends presented so far suggest that the modified coatings of the cylinder are able to enhance the physical effect responsible for noise mitigation. To shed light on the nature of the generated sound sources, the frequency spectra presented at a reference distance of 1 m are scaled with the sixth power of U_∞, which is known to be related to a dipolar sound directivity[31]. The results are reported in Figs. 5 and 6 for the modifications in the presence and absence of the porous coating, respectively. For the former, a good collapse of the sound-pressure levels is found for all the cylinder configurations and for most of the frequency spectrum, in agreement with the outcomes of the scaling analysis carried out by Zamponi *et al.* [15] on the baseline and the cylinder uniformly coated with the 10 PPI metal foam. Similar findings are obtained when the solid and porous inserts are connected to the bare cylinder (Figs. 6a and 6b), suggesting that the noise-generation mechanism is unchanged.

The outcome of this investigation confirms that sound waves acquired by the microphone are those scattered by the cylinder surface, which, as mentioned in Section I, feature dipolar directivity. However, this trend is not maintained when the tails are integrated into the baseline design. In this case, the optimal scaling factor of the noise spectra for the flow velocity is found to be closer to 5, implying that noise may be produced by the scattering of the turbulent boundary layer at the trailing edge of the component [32].

IV. Concluding remarks

This study demonstrates that the proposed innovative designs for cylinder coatings based on the alteration of the sound diffraction are effective in reducing the corresponding flow-induced noise. Inexpensive and light modifications of a porous cover, in the form of inserts or tails integrated into the porous material, can yield additional attenuation of up to 10 dB throughout the frequency spectrum. In a previous study by the authors, it was demonstrated that the aerodynamic noise radiated by the flow past a cylinder is dominated by the scattering of the quadrupolar source originating at the vortex-shedding onset location by the body surface, which is dipolar in nature. The farther from the surface this position is, the less efficient the sound diffraction will be. This mechanism is at the basis of the noise reduction achievable by a porous coating of the cylinder. The presence of a component in the leeward part of the cover that better guides the internal flow around the body results in a further downstream displacement of the shedding-instability outbreak, i.e., better sound mitigation. In some instances, such as when the solid tail is integrated into the porous coating, the tonal peak associated with the vortex shedding in the noise spectra is found to be almost completely suppressed. Interestingly, a consistent attenuation of up to 10 dB with respect to the baseline is obtained when the same components are connected to the cylinder, without the presence of the porous layer. Such an effect is induced by the same mechanism described above. Besides constituting an effective passive noise-control strategy, this solution potentially contributes to reducing the drag force produced by the body, opening interesting scenarios for industrial applications. Future flow measurements will verify this hypothesis.

Finally, the results discussed in this paper show that an exhaustive understanding of the sound-reduction mechanisms of a porous cover of the cylinder can lead to novel technological solutions for abating the corresponding flow-induced noise. However, no optimization of the coating modifications has been attempted yet, leaving considerable room for improvement of their aeroacoustic performance. In this regard, the recent advancements in additive-manufacturing techniques can offer the perfect framework for designing non-uniform porous covers that are able to maximize the downstream source shift.

Acknowledgments

References

[1] Strouhal, V., "Ueber eine besondere Art der Tonerregung," *Annalen der Physik und Chemie*, Vol. 241, No. 10, 1878, pp. 216–251. https://doi.org/10.1002/andp.18782411005.

[2] Rashidi, S., Hayatdavoodi, M., and Esfahani, J., "Vortex shedding suppression and wake control: A review," *Ocean Engineering*, Vol. 126, 2016, pp. 57–80. https://doi.org/10/f9bv56.

[3] Sueki, T., Takaishi, T., Ikeda, M., and Arai, N., "Application of porous material to reduce aerodynamic sound from bluff bodies," *Fluid Dynamics Research*, Vol. 42, No. 1, 2010, p. 015004. https://doi.org/10.1088/0169-5983/42/1/015004.

[4] Naito, H., and Fukagata, K., "Numerical simulation of flow around a circular cylinder having porous surface," *Physics of Fluids*, Vol. 24, No. 11, 2012, p. 117102. https://doi.org/10.1063/1.4767534.

[5] Liu, H., Wei, J., and Qu, Z., "Prediction of aerodynamic noise reduction by using open-cell metal foam," *Journal of Sound and Vibration*, Vol. 331, No. 7, 2012, pp. 1483–1497. https://doi.org/10.1016/j.jsv.2011.11.016.

[6] Aguiar, J., Yao, H., and Liu, Y., "PASSIVE FLOW/NOISE CONTROL OF A CYLINDER USING METAL FOAM," *The 23rd International Congress on Sound and Vibration*, The International Institute of Acoustics and Vibration, 2016, p. 9.

[7] Showkat Ali, S., Liu, X., and Azarpeyvand, M., "Bluff Body Flow and Noise Control Using Porous Media," *22nd AIAA/CEAS Aeroacoustics Conference*, American Institute of Aeronautics and Astronautics, Lyon, France, 2016. https://doi.org/10.2514/6.2016-2754.

[8] Geyer, T., and Sarradj, E., "Circular cylinders with soft porous cover for flow noise reduction," *Experiments in Fluids*, Vol. 57, No. 3, 2016, p. 30. https://doi.org/10.1007/s00348-016-2119-7.

[9] Geyer, T., "Experimental evaluation of cylinder vortex shedding noise reduction using porous material," *Experiments in Fluids*, Vol. 61, No. 7, 2020, p. 153. https://doi.org/10.1007/s00348-020-02972-0.

[10] Arcondoulis, E., Liu, Y., Li, Z., Yang, Y., and Wang, Y., "Structured Porous Material Design for Passive Flow and Noise Control of Cylinders in Uniform Flow," *Materials*, Vol. 12, No. 18, 2019, p. 2905. https://doi.org/10.3390/ma12182905.

[11] Arcondoulis, E., Ragni, D., Rubio Carpio, A., Avallone, F., Liu, Y., Yang, Y., and Li, Z., "The internal and external flow fields of a structured porous coated cylinder and implications on flow-induced noise," *25th AIAA/CEAS Aeroacoustics Conference*, American Institute of Aeronautics and Astronautics, Delft, The Netherlands, 2019. https://doi.org/10.2514/6.2019-2648.

[12] Arcondoulis, E., Geyer, T., and Liu, Y., "An investigation of wake flows produced by asymmetrically structured porous coated cylinders," *Physics of Fluids*, Vol. 33, No. 3, 2021, p. 037124. https://doi.org/10.1063/5.0042496.

[13] Arcondoulis, E., Geyer, T., and Liu, Y., "An acoustic investigation of non-uniformly structured porous coated cylinders in uniform flow," *The Journal of the Acoustical Society of America*, Vol. 150, No. 2, 2021, pp. 1231–1242. https://doi.org/10/gpdzqs.

[14] Bathla, P., and Kennedy, J., "3D Printed Structured Porous Treatments for Flow Control around a Circular Cylinder," *Fluids*, Vol. 5, No. 3, 2020, p. 136. https://doi.org/10.3390/fluids5030136.

[15] Zamponi, R., Avallone, F., Ragni, D., and van der Zwaag, S., "On the Aerodynamic-Noise Sources in a Circular Cylinder Coated with Porous Materials," *28th AIAA/CEAS Aeroacoustics 2022 Conference*, American Institute of Aeronautics and Astronautics, Southampton, UK, 2022. https://doi.org/10.2514/6.2022-3042.

[16] Gloerfelt, X., Pérot, F., Bailly, C., and Juvé, D., "Flow-induced cylinder noise formulated as a diffraction problem for low Mach numbers," *Journal of Sound and Vibration*, Vol. 287, No. 1-2, 2005, pp. 129–151. https://doi.org/10.1016/j.jsv.2004.10.047.

[17] Merino-Martínez, R., Rubio Carpio, A., Lima Pereira, L., van Herk, S., Avallone, F., Ragni, D., and Kotsonis, M., "Aeroacoustic design and characterization of the 3D-printed, open-jet, anechoic wind tunnel of Delft University of Technology," *Applied Acoustics*, Vol. 170, 2020, p. 107504. https://doi.org/10.1016/j.apacoust.2020.107504.

[18] Porteous, R., Moreau, D., and Doolan, C., "A review of flow-induced noise from finite wall-mounted cylinders," *Journal of Fluids and Structures*, Vol. 51, 2014, pp. 240–254. https://doi.org/10.1016/j.jfluidstructs.2014.08.012.

[19] Rubio Carpio, A., Merino Martínez, R., Avallone, F., Ragni, D., Snellen, M., and van der Zwaag, S., "Experimental characterization of the turbulent boundary layer over a porous trailing edge for noise abatement," *Journal of Sound and Vibration*, Vol. 443, 2019, pp. 537–558. https://doi.org/10.1016/j.jsv.2018.12.010.

[20] Ingham, D., and Pop, I., *Transport phenomena in porous media*, Elsevier, 1998. https://doi.org/10.1016/B978-0-08-042843-7.X5000-4.

[21] Baril, E., Mostafid, A., Lefebvre, L., and Medraj, M., "Experimental Demonstration of Entrance/Exit Effects on the Permeability Measurements of Porous Materials," *Advanced Engineering Materials*, Vol. 10, No. 9, 2008, pp. 889–894. https://doi.org/10.1002/adem.200800142.

[22] Dukhan, N., and Patel, K., "Effect of sample's length on flow properties of open-cell metal foam and pressure-drop correlations," *Journal of Porous Materials*, Vol. 18, No. 6, 2011, pp. 655–665. https://doi.org/10.1007/s10934-010-9423-z.

[23] Welch, P., "The use of fast Fourier transform for the estimation of power spectra: A method based on time averaging over short, modified periodograms," *IEEE Transactions on Audio and Electroacoustics*, Vol. 15, No. 2, 1967, pp. 70–73. https://doi.org/10.1109/TAU.1967.1161901.

[24] Brandt, A., *Noise and vibration analysis: signal analysis and experimental procedures*, John Wiley & Sons, 2011.

[25] Zamponi, R., Satcunanathan, S., Moreau, S., Ragni, D., Meinke, M., Schröder, W., and Schram, C., "On the role of turbulence distortion on leading-edge noise reduction by means of porosity," *Journal of Sound and Vibration*, Vol. 485, 2020, p. 115561. https://doi.org/10.1016/j.jsv.2020.115561.

[26] Tamaro, S., Zamponi, R., Ragni, D., Teruna, C., and Schram, C., "Experimental investigation of turbulent coherent structures interacting with a porous airfoil," *Experiments in Fluids*, Vol. 62, 2021, p. 94. https://doi.org/10.1007/s00348-021-03170-2.

[27] Anderson, E. A., and Szewczyk, A. A., "Effects of a splitter plate on the near wake of a circular cylinder in 2 and 3-dimensional flow configurations," *Experiments in Fluids*, Vol. 23, No. 2, 1997, pp. 161–174. https://doi.org/10.1007/s003480050098.

[28] Zamponi, R., Moreau, S., and Schram, C., "Rapid distortion theory of turbulent flow around a porous cylinder," *Journal of Fluid Mechanics*, Vol. 915, 2021, p. A27. https://doi.org/10.1017/jfm.2021.8.

[29] Zamponi, R., Satcunanathan, S., Moreau, S., Meinke, M., Schröder, W., and Schram, C., "Effect of porosity on Curle's dipolar sources on an aerofoil in turbulent flow," *Journal of Sound and Vibration*, Vol. 542, 2023, p. 117353. https://doi.org/10.1016/j.jsv.2022.117353.

[30] Zamponi, R., Van de Wyer, N., and Schram, C., "Experimental Investigation of Airfoil Turbulence-Impingement Noise Reduction Using Porous Treatment," *25th AIAA/CEAS Aeroacoustics Conference*, American Institute of Aeronautics and Astronautics, Delft, The Netherlands, 2019. https://doi.org/10.2514/6.2019-2649.

[31] Curle, N., "The influence of solid boundaries upon aerodynamic sound," *Proceedings of the Royal Society of London. Series A. Mathematical and Physical Sciences*, Vol. 231, No. 1187, 1955, pp. 505–514. https://doi.org/10.1098/rspa.1955.0191.

[32] Ffowcs Williams, J., and Hall, L., "Aerodynamic sound generation by turbulent flow in the vicinity of a scattering half plane," *Journal of Fluid Mechanics*, Vol. 40, No. 04, 1970, p. 657. https://doi.org/10.1017/S0022112070000368.